

tion of antagonistic muscles has been demonstrated are the locust escape jump [R. H. J. Brown, *Nature* 214, 939 (1967)] and the predatory strike of the dragonfly larva [Y. Tanaka and M. Hisada, *J. Exp. Biol.* 88, 1 (1980)] or of the mantid shrimp [M. Burrows, see (7)].

19. We thank S. O. Andersen for his advice suggesting that the tendon between the mandible and its closer muscle would be the most probable region in which to find energy-storing materials such as resilin. We also thank the German Institute for the Scientific Film (IWF), where the high-speed cine-

matography was carried out. Supported by funds from the Deutsche Forschungsgemeinschaft (Leibniz Preis to B.H., SFB 251/project 18, and Gr 933/3).

15 June 1993; accepted 12 August 1993

FMR1 Protein: Conserved RNP Family Domains and Selective RNA Binding

Claude T. Ashley Jr., Keith D. Wilkinson, Daniel Reines, Stephen T. Warren*

Fragile X syndrome is the result of transcriptional suppression of the gene *FMR1* as a result of a trinucleotide repeat expansion mutation. The normal function of the *FMR1* protein (FMRP) and the mechanism by which its absence leads to mental retardation are unknown. Ribonucleoprotein particle (RNP) domains were identified within FMRP, and RNA was shown to bind in stoichiometric ratios, which suggests that there are two RNA binding sites per FMRP molecule. FMRP was able to bind to its own message with high affinity (dissociation constant = 5.7 nM) and interacted with approximately 4 percent of human fetal brain messages. The absence of the normal interaction of FMRP with a subset of RNA molecules might result in the pleiotropic phenotype associated with fragile X syndrome.

Fragile X syndrome is an X-linked dominant disorder with reduced penetrance that occurs at a frequency of approximately 0.5 to 1.0 per 1000 males and 0.2 to 0.6 per 1000 females (1). Fully penetrant males exhibit moderate mental retardation along with a phenotype consisting of macroorchidism (enlarged testes), subtle facial dysmorphism, and mild connective tissue abnormalities (2). Female patients typically are less severely affected, showing little or no somatic signs and only borderline to mild mental retardation. The molecular basis of fragile X syndrome has been attributed to the expansion of an unstable CCG trinucleotide repeat in the 5' untranslated region of the gene *FMR1* (3, 4).

In fragile X syndrome, when the size of the CCG repeat is in the affected range beyond 230 repeats, the *FMR1* gene is methylated; this methylation results in transcriptional silencing (5). The absence of *FMR1* message and its encoded protein, FMRP, is believed responsible for the phenotype of the fragile X syndrome. In addition to the common mutational change of repeat expansion, three variant patients with the clinical presentation of fragile X syndrome have been reported: two males with large deletions encompassing the *FMR1* locus and a severely affected male with a *FMR1* Ile³⁰⁴→Asn missense mutation (6).

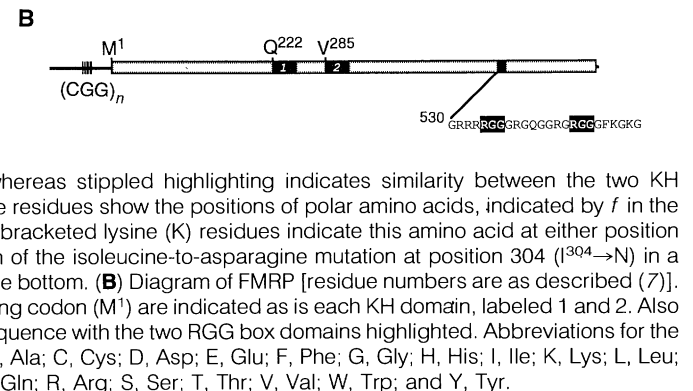
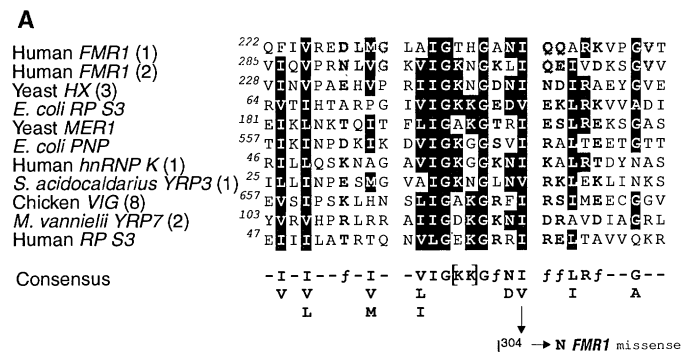
Alternative splicing generates several isoforms of FMRP with a major species of 69 kD (7). Although predominantly cytoplasmic, occasional nuclear localization is observed (8). In situ hybridization with *FMR1* mRNA reveals widespread but not ubiquitous expression with abundant message present in the testes and in neurons in the brain (9).

Initial analyses of *FMR1* and the pre-

dicted protein sequence revealed little sequence similarity to known proteins or motifs. Further analyses of the human and mouse genes, particularly with the use of searches of limited regions of 200 to 400 amino acids in length, revealed two similar regions of FMRP that also were similar to 6 repetitive domains in the yeast protein HX and 14 domains of the chicken gene *vigillin* (*VIG*) (10). Alignments of these amino acid sequences and a resulting profile search revealed a number of proteins containing 1 to 14 repeats of an uninterrupted, 30–amino acid domain (Fig. 1A). Proteins containing this domain, termed KH domains, are believed to constitute a ribonucleoprotein (RNP) family (11) that includes *mer1*, a yeast protein involved in meiosis-specific alternative splicing (12); bacterial polynucleotide phosphorylase, which binds RNA and has phosphorolysis activity (13); and the highly conserved ribosomal protein S3 (RP S3) (14). Thus, most functional aspects of RNA-protein interactions are represented among KH domain-containing proteins, including RNA catalysis, message processing, and translation.

The two KH domains of FMRP reside in the middle of the protein (Fig. 1B), a

Fig. 1. Location and homologies of RNP family domains in FMRP. (A) Alignment (27) of the amino acid sequences that make up the KH domains of FMRP and several other proteins and the corresponding consensus sequence. Numbers in parentheses indicate the particular domain shown for the proteins that have multiple KH domains, and the number preceding the first residue indicates that position in the corresponding protein. Dark highlighting indicates similarities among all proteins, whereas stippled highlighting indicates similarity between the two KH domains of FMRP. Boldface residues show the positions of polar amino acids, indicated by *f* in the consensus sequence. The bracketed lysine (K) residues indicate this amino acid at either position in the domain. The position of the isoleucine-to-asparagine mutation at position 304 (I³⁰⁴→N) in a patient (6) is indicated at the bottom. (B) Diagram of FMRP [residue numbers are as described (7)]. The CCG repeat and initiating codon (M¹) are indicated as is each KH domain, labeled 1 and 2. Also shown is the amino acid sequence with the two RGG box domains highlighted. Abbreviations for the amino acid residues are: A, Ala; C, Cys; D, Asp; E, Glu; F, Phe; G, Gly; H, His; I, Ile; K, Lys; L, Leu; M, Met; N, Asn; P, Pro; Q, Gln; R, Arg; S, Ser; T, Thr; V, Val; W, Trp; and Y, Tyr.



C. T. Ashley Jr., K. D. Wilkinson, D. Reines, Department of Biochemistry, Emory University School of Medicine, Atlanta, GA 30322.

S. T. Warren, Howard Hughes Medical Institute and Departments of Biochemistry and Pediatrics, Emory University School of Medicine, Atlanta, GA 30322.

*To whom correspondence should be addressed.

region not involved in alternative splicing (7). Furthermore, the two FMRP domains show 100% amino acid identity among the human, mouse, and chicken *FMR1* homologs (15). In the single patient with severe fragile X syndrome that was a result of a missense *FMR1* mutation (6), this mutation was in an invariant isoleucine in the 20th position of the second KH domain (Fig. 1A). In addition, FMRP shows two RGG (Arg-Gly-Gly) boxes toward the carboxyl end. RGG boxes are another distinct RNP motif found in heterogeneous nuclear RNP K (hnRNP K) and nucleolar proteins (16).

To biochemically establish and characterize RNA binding by FMRP, we measured ³⁵S-labeled FMRP bound to biotinylated RNA (17). The ³⁵S-FMRP was translated in vitro from a full-length *FMR1* complementary DNA (cDNA) (18), which resulted in a 69-kD protein as well as smaller, secondary products of the reaction (Fig. 2A, lane 1). *FMR1* RNA was transcribed in vitro from the same cDNA with the T3 (sense) or T7 (antisense) promoter in the presence of biotin-uridine 5'-triphosphate (UTP) (19). Biotinylated RNA was mixed with the in vitro translation reaction and captured with streptavidin-linked magnetic beads. After three washes, bound protein was released by denaturation and assayed by SDS-polyacrylamide gel electrophoresis (PAGE) and fluorography. A known RNA binding protein, Brome mosaic virus (BMV) RNA-dependent RNA polymerase, was captured by this assay (Fig. 2A), whereas no binding was observed with a fourfold higher molar concentration of the 15-kD parathyroid hormone precursor protein, which does not associate with RNA (20). Only the 69-kD protein, corresponding to the mass of FMRP, was captured from the *FMR1* in vitro translation mix by the biotinylated RNA. Hydroxylamine cleavage of this 69-kD protein, released from the biotinylated RNA, resulted in a doublet band

at approximately 34 kD. Two bands of 33 and 34 kD are predicted based on the FMRP sequence, which confirms that this species is FMRP (21).

The FMRP was able to bind to sense or antisense *FMR1* RNA (Fig. 2B). Experiments were performed in the presence of a 62-fold excess of transfer RNA, suggesting that the protein specifically binds to unstructured RNA, perhaps allowing access to the sugar-phosphate backbone and unpaired bases for protein interaction. Ribonuclease (RNase) treatment before streptavidin exposure as well as use of nonbiotinylated RNA resulted in no capture of FMRP (Fig. 2B). FMRP binds strongly to single-stranded DNA but to a lesser extent to double-stranded DNA (Fig. 2B), which is similar to the binding of other RNP family proteins (22). To test whether FMRP binds to all RNA species, we pooled a human fetal brain plasmid cDNA library (23) and performed in vitro transcription in the presence of biotin-UTP. A complex mixture of RNAs (average size of 700 base pairs) was produced, some of which allowed the capture of FMRP (Fig. 2B, lane 4). However, much less RNA binding was observed with the pooled RNAs as compared with that in the presence of *FMR1* RNA, even with a sixfold molar excess of the former over the latter. Thus, it appears that FMRP is not a general, nonspecific RNA binding protein but rather exhibits some degree of specificity for the RNA species with which it interacts.

As an independent measure of FMRP binding to RNA, a monoclonal antibody (D44), which binds specifically to RNA (24), was used (Fig. 2C). D44 immunoprecipitation of nonbiotinylated RNA with bound FMRP was achieved when protein A-linked agarose beads were used to capture the complex. RNase treatment abolished FMRP capture by this assay as well.

Estimates of the strength of the interaction of FMRP with RNA were next ob-

tained. Protein titration studies (Fig. 3) demonstrate saturation behavior of FMRP binding to 80 ng of RNA. At saturation, 3 nM FMRP was bound, as estimated by direct scintillation counting of the bound FMRP (25). Because the RNA concentration was held constant at 6 nM, a 2:1 stoichiometry of RNA:protein was obtained. Similar studies with RNA from human fetal brain cDNA transcribed in vitro also displayed saturation, but only 1.5 nM FMRP was bound. Considering that the brain RNA was held at a higher concentration of 34 nM, a stoichiometry of approximately 27:1 (RNA:protein) was determined, which suggests that there was selective FMRP binding to approximately 4% by mass of the human fetal brain message. Because *FMR1* is estimated to account for less than 0.01% of this pool, these data demonstrate FMRP interaction with messages of other human genes.

Biotinylated RNA transcripts from randomly chosen human fetal brain cDNA clones were tested for selective FMRP binding. Analysis of 12 clones identified two that produced RNA that bound to FMRP (Fig. 4). Insert size appeared unrelated to binding ability, and preliminary sequence analysis of those clones whose RNA bound did not reveal any obvious homology to *FMR1* cDNA nor to any database sequence. Thus, selective RNA binding of

Fig. 2. Binding of RNA to FMRP. (A) Validation of the biotinylated RNA binding assay (28) with in vitro-translated FMRP (lanes 1 and 2), BMV RNA-dependent polymerase (positive control, lanes 3 and 4), and parathyroid hormone precursor protein (negative control, lanes 5 and 6). The complete in vitro translation mix of each is shown before (lanes 1, 3, and 5) and after (lanes 2, 4, and 6) binding to in vitro-transcribed biotinylated *FMR1* RNA (19). (B) Nucleic acid binding properties of 2 μ l of in vitro-translated FMRP (lane 1) with 80 ng of various nucleic acids: lanes 2 and 3, biotinylated and nonbiotinylated, respectively, *FMR1* RNA (sense); lanes 4 and 5, biotinylated and nonbiotinylated, respectively, human fetal brain RNA pool (23); lane 6, biotinylated *FMR1* RNA (antisense); lanes 7 and 8, double- and single-stranded, respectively, *FMR1* DNA (29); and lane 9, biotinylated *FMR1* RNA (sense) treated with RNase (1 μ g/ μ l of RNase A and 1 U of T1 RNase) before streptavidin capture. (C) Co-immunoprecipitation of 2 μ l of in vitro-translated FMRP and nonbiotinylated *FMR1* RNA (30) in the presence (lane 1) or absence (lane 2) of the D44 RNA antibody (25). Lane 3, precipitated FMRP in the presence of antibody and RNase (1 μ g/ μ l of RNase A and 1 U of RNase T1).

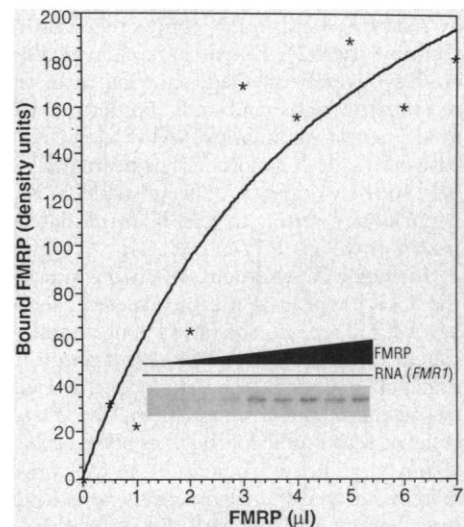
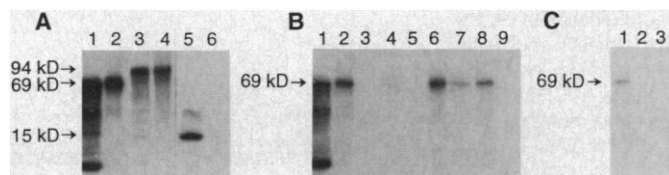
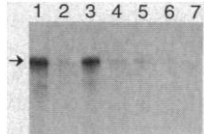


Fig. 3. Titration of FMRP with a constant amount of biotinylated *FMR1* RNA. Amounts of in vitro-translated FMRP ranging from 0 to 7 μ l were incubated with 80 ng of biotinylated *FMR1* RNA, and captured protein was eluted and analyzed as described. The fluorogram of the individual binding reactions (inset) was subjected to densitometry, and amounts of bound protein inferred from the density of the individual bands (y axis) were plotted versus the amount of in vitro-translated FMRP (x axis) used (26). Asterisks denote individual data points.

FMRP is substantiated, and further analysis of these clones, in conjunction with analysis of *FMR1*, should allow recognition of any structural RNA determinants required for FMRP binding.

As would be predicted for saturable binding of FMRP to RNA, competition was observed with nonbiotinylated RNA (Fig. 5A). Saturable binding was further substantiated by a series of analyses in which the amount of labeled FMRP was kept constant

Fig. 4. Selectivity of FMRP binding to random human fetal brain messages. Plasmid DNA prepared from individual colonies isolated from the human fetal brain library (23) was used as a template for in vitro transcription reactions carried out in the presence of biotin UTP (19). The binding of in vitro-translated FMRP to 80 ng of biotinylated RNA from six representative brain clones (of twelve tested) is shown [lane 2, clone 39.1 (0.9-kb insert); lane 3, 19.1 (0.7 kb); lane 4, 19.2 (1.0 kb); lane 5, 19.3 (1.0 kb); lane 6, 3.2 (2.8 kb); and lane 7, 3.3 (0.8 kb)] as compared to 80 ng of biotinylated *FMR1* RNA alone (lane 1). RNA transcribed from clone 19.1 (lane 3) demonstrated binding equivalent to that of *FMR1* RNA, whereas RNA produced from the remaining clones demonstrated little or no interaction with FMRP. Arrow indicates 69-kD band.



and the amount of biotinylated *FMR1* RNA or biotinylated brain RNA was increased (Fig. 5B). Curve fitting with a simple binding equation (26) resulted in an apparent dissociation constant (K_d) of 5.7 nM for *FMR1* RNA. When human fetal brain RNA was used, an apparent K_d of 39 nM was obtained. These results were confirmed by direct scintillation counting of bound 35 S-FMRP. Substitution of the value for the estimated K_d (5.7 nM) into the equation that described the competition data (Fig. 5A) produced an estimated inhibition constant (K_i) of 12.4 nM. The difference in estimated values for K_d and K_i may reflect either that the biotinylated RNA acts as a better ligand than nonbiotinylated RNA or that there are two RNA binding sites per protein molecule. The latter possibility would reduce the apparent binding constant because biotinylated RNA bound to either or both sites would result in capture of the FMRP molecule by streptavidin. Because the stoichiometry at saturation suggested a 2:1 *FMR1* RNA:FMRP ratio, this possibility is likely. One may also speculate that either the KH or RGG domains, each present twice in FMRP, are directly binding RNA.

The demonstration that FMRP is an RNA binding protein suggests an avenue of further inquiry as to the precise function of FMRP. Given that the major neurological

phenotype of fragile X syndrome is mental retardation, these data provide a means to explore the biochemical basis of cognitive function in humans as well as the pathophysiology of fragile X syndrome. The observation that FMRP interacts with a selective, but substantial, fraction of human brain RNA suggests that other genes, whose products may vary in the absence of FMRP, could play a consequential role in the pleiotropic phenotype of fragile X syndrome.

REFERENCES AND NOTES

1. W. T. Brown, *Am. J. Hum. Genet.* **47**, 175 (1990); S. L. Sherman *et al.*, *Ann. Hum. Genet.* **48**, 21 (1984).
2. M. G. Butler, T. Mangrum, R. Gupta, D. N. Singh, *Clin. Genet.* **39**, 347 (1991).
3. A. M. J. H. Verkerk *et al.*, *Cell* **65**, 905 (1991); I. Oberlé *et al.*, *Science* **252**, 1097 (1991); E. J. Kremer *et al.*, *ibid.*, p. 1711; A. Vincent *et al.*, *Nature* **349**, 624 (1991).
4. Y. H. Fu *et al.*, *Cell* **67**, 1047 (1991); S. Yu *et al.*, *Science* **252**, 1179 (1991).
5. M. Pieretti *et al.*, *Cell* **66**, 817 (1991); J. S. Sutcliffe *et al.*, *Hum. Mol. Genet.* **1**, 397 (1992).
6. D. Wohlrlé *et al.*, *Am. J. Hum. Genet.* **51**, 299 (1992); A. K. Gideon *et al.*, *Nature Genet.* **1**, 341 (1992); K. De Bouille *et al.*, *ibid.* **3**, 31 (1993).
7. C. T. Ashley *et al.*, *Nature Genet.* **4**, 244 (1993).
8. C. Verheij *et al.*, *Nature* **363**, 722 (1993).
9. H. L. Hinds *et al.*, *Nature Genet.* **3**, 36 (1993).
10. A. Delahodde, A. M. Becam, J. Perea, C. Jacq, *Nucleic Acids Res.* **14**, 9213 (1986); C. Schmidt *et al.*, *Eur. J. Biochem.* **206**, 625 (1992).
11. H. Siomi, M. J. Matunis, W. M. Michael, G. Dreyfuss, *Nucleic Acids Res.* **21**, 1193 (1993).
12. J. Engebrecht and G. S. Roeder, *Mol. Cell. Biol.* **10**, 2379 (1990).
13. P. Regnier, M. Grunberg-Manago, C. Portier, *J. Biol. Chem.* **262**, 63 (1987).
14. X. T. Zhang, Y.-M. Tan, Y. H. Tan, *Nucleic Acids Res.* **18**, 6689 (1990); D. Brauer and R. Roming, *FEBS Lett.* **106**, 352 (1979).
15. D. Price and S. T. Warren, unpublished material.
16. I. W. Mattaj, *Cell* **73**, 837 (1993).
17. W. C. Boelens *et al.*, *ibid.* **72**, 881 (1993).
18. The full-length murine *FMR1* cDNA (4256 base pairs) Mc 2.17 described in Ashley *et al.* (7) was linearized for transcription with either Nsi I (sense) or Not I (antisense). In vitro transcription was carried out with the T3-T7 in vitro transcription kit (Stratagene). In vitro translation was in rabbit reticulocyte lysates of the In Vitro Express kit (Stratagene).
19. Biotinylated RNA (*FMR1* and *HFB*) was synthesized in the presence of biotinylated ribonucleotide uridine triphosphate (rUTP) (ENZO, Farmingdale, NY) as described (17) at a molar ratio of 1:10 (biotinylated rUTP:rUTP).
20. BMV RNA-dependent RNA polymerase [C. C. Kao, R. Quadt, R. P. Hershberger, P. Ahlquist, *J. Virol.* **66**, 6322 (1992)] was synthesized from RNA purchased from Promega. Only the 94-kD RNA-dependent RNA polymerase was translated in the In Vitro Express system (Stratagene). Parathyroid hormone precursor was translated from RNA included in the In Vitro Express system.
21. Captured protein from four standard binding reactions (80 ng of biotinylated *FMR1* RNA and 2 μ l of in vitro-translated FMRP) was resuspended in 100 μ l of 2 M hydroxylamine HCl in 6 M guanidine HCl (pH 9.0). After a 90-min incubation at 45°C, the cleaved protein was released by heating (3 min at 100°C) and analyzed by SDS-PAGE, as described (28). Predicted hydroxylamine cleavage sites at residues 13, 301, and 612 of the FMRP sequence (7) resulted in a doublet band at 34 kD.
22. M. J. Matunis, W. M. Michael, G. Dreyfuss, *Mol. Cell. Biol.* **12**, 164 (1992).

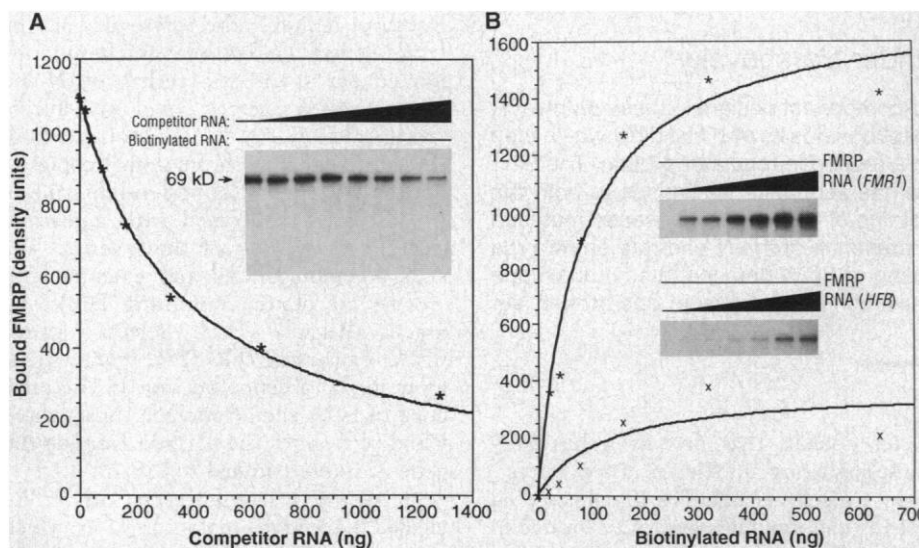


Fig. 5. Characterization of FMRP binding to *FMR1* RNA. **(A)** Competition of FMRP binding by addition of nonbiotinylated *FMR1* RNA. Constant amounts of FMRP (2 μ l) and biotinylated *FMR1* RNA (80 ng) were incubated with increasing amounts of nonbiotinylated *FMR1* RNA (0 to 1280 ng), and captured FMRP was analyzed by SDS-PAGE and fluorography (inset). Densitometry was used to estimate amounts of bound protein, and bound FMRP (y axis) was plotted (26) against amounts of nonbiotinylated *FMR1* RNA (x axis). Asterisks denote individual data points. **(B)** RNA titrations of FMRP binding with increasing amounts of *FMR1* RNA or human fetal brain (*HFB*) RNA. A constant amount of FMRP (2 μ l) was incubated in the presence of increasing amounts of either biotinylated *FMR1* RNA (asterisks) or biotinylated *HFB* RNA (x) ranging from 0 to 640 ng, and the FMRP captured was analyzed by SDS-PAGE followed by fluorography. Fluorograms (insets) were scanned by densitometry, and the relative amount of bound FMRP (y axis) was plotted (26) versus the amount of biotinylated RNA added (x axis).

23. The human fetal brain plasmid cDNA library (Invitrogen) was amplified in toto, and cesium-purified plasmid DNA was linearized at the Xba I site. In vitro transcription was performed from a T7 promoter as described (18, 19).
24. D. Eilat, M. Hochberg, R. Fischel, R. Laskov, *Proc. Natl. Acad. Sci. U.S.A.* **79**, 3818 (1982).
25. The specific activity of [³⁵S]methionine used was 1275 Ci/mmol. Given the molecular weight (69 kD) and that nine methionines existed in FMRP (7), the expected number of disintegrations per minute per mole of protein was calculated and adjusted according to the predetermined efficiency of counting (69%) for the isotope. The number of moles of bound protein was determined by dividing the observed counts per minute of bound protein at saturation by the expected disintegrations per minute per mole; the concentration value given was determined by dividing by the reaction volume.
26. The standard binding equation used was $b = b_m \frac{[L]}{K_d + [L]}$, where b is the amount of protein bound, b_m is the maximum amount bound, $[L]$ is the concentration of ligand, and K_d is the dissociation constant. Maximum amounts of bound protein were determined from direct scintillation counting of binding reactions performed in triplicate at constant amounts of ligand. Amounts of bound protein were determined either through direct scintillation counting or densitometric analysis of fluorograms. Data points were fit to this equation with the nonlinear least squares method furnished in the plotting program Delta Graph (Deltapoint, Inc., Monterey, CA), and equations were solved for the apparent K_d . A variation of this equation, $b = b_m \frac{[L]}{K_d(1 + [I]/K_i) + [L]}$ (where $[I]$ = concentration of inhibitor), was used to fit the RNA competition curve and to solve for K_i .
27. M. Gribskov, R. Luethy, D. Eisenberg, *Methods Enzymol.* **183**, 146 (1989).
28. Biotinylated RNA binding assays were performed as described by Boelens *et al.* (17), except that magnetic beads with conjugated streptavidin (Dynal) were used. Captured material was resuspended in 20 μ l of 1 \times SDS sample buffer, and bound protein was eluted by boiling for 10 min and resolved by SDS-PAGE. The 12% SDS-polyacrylamide gels were soaked for 30 min in destain solution (7.5% methanol and 10% acetic acid), followed by 1 hour in 1 M salicylate solution (1 M salicylate, 30% methanol, and 3.0% glycerol). Gels were then dried and exposed at -80°C with an intensifying screen for 24 to 72 hours.
29. Biotinylated DNA was prepared with a nick translation kit (Amersham) in the presence of biotinylated deoxythymidine triphosphate (dTTP) (BRL) at an equal molar ratio with dTTP and passed through a G-50 Sephadex spin column (Boehringer Mannheim) followed by precipitation. Single-strand DNA was obtained by heat denaturation of the product above.
30. Immunoprecipitations were carried out in the presence of 2 μ l of in vitro-translated FMRP, D44 (20 ng/ μ l), and 80 ng of nonbiotinylated FMRP RNA by means of the same protocol as used in the biotinylated RNA binding assays (17). RNA molecules bound to antibody and FMRP were captured with protein A that had been linked to agarose beads (BRL; an amount equivalent to 20 μ l). After centrifugation, pellets were washed as described (17), resuspended in 20 μ l of 1 \times SDS buffer, and resolved by SDS-PAGE.
31. Supported by NIH grant HD20521 (S.T.W.). C.T.A. is a predoctoral fellow of the March of Dimes Birth Defects Foundation, and S.T.W. is an Investigator of the Howard Hughes Medical Institute.

21 July 1993; accepted 30 August 1993

A Yeast Protein Similar to Bacterial Two-Component Regulators

Irene M. Ota and Alexander Varshavsky*

Many bacterial signaling pathways involve a two-component design. In these pathways, a sensor kinase, when activated by a signal, phosphorylates its own histidine, which then serves as a phosphoryl donor to an aspartate in a response regulator protein. The *Slr1* protein of the yeast *Saccharomyces cerevisiae* has sequence similarities to both the histidine kinase and the response regulator proteins of bacteria. A missense mutation in *SLN1* is lethal in the absence but not in the presence of the N-end rule pathway, a ubiquitin-dependent proteolytic system. The finding of *SLN1* demonstrates that a mode of signal transduction similar to the bacterial two-component design operates in eukaryotes as well.

In bacteria, a broad spectrum of responses to an often rapidly changing environment is mediated by mechanistically similar pathways known as two-component systems. The functions of two-component pathways include chemotaxis, sporulation, osmoregulation, transformation competence, virulence, and responses to changes in the sources of carbon, nitrogen, oxygen, and phosphorus (1-3). The sensor component of these systems is often an integral membrane protein containing a cytosolic trans-

mitter domain that acts as a histidine-phosphorylating autokinase, when activated by a specific signal. The signal is sensed by a distinct input domain, often located in the periplasmic space. The histidine-linked phosphoryl group of an activated transmitter is transferred to an aspartate in the receiver domain of a response regulator protein, the second component of the pathway. Receiver phosphorylation regulates the activity of its output module, which is often a DNA-binding domain (1-3).

Although two-component pathways are common in bacteria, evidence for their existence in eukaryotes has been scarce. A protein kinase from rat mitochondria has

sequence similarities to bacterial histidine kinases; however, in vitro it phosphorylates a Ser residue (4). Another eukaryotic candidate is phytochrome, a plant regulatory protein that has weak but potentially significant similarities to the sequences of bacterial histidine kinases (5). Histidine kinase activity has been detected in extracts from *S. cerevisiae* and other eukaryotic cells (6).

This report describes the *S. cerevisiae* *SLN1* gene which encodes a 134-kD product with strong sequence similarities to both the transmitter and receiver domains of the bacterial two-component regulators. We found *SLN1* while studying the N-end rule, a relation between the in vivo half-life of a protein and the identity of its N-terminal residue (7, 8). The N-end rule is a consequence of a set of ubiquitin-dependent degradation signal called N-degrons (9). Ubiquitin is a protein whose covalent conjugation to other proteins plays a role in a number of cellular processes, primarily through routes that involve protein degradation (8). In *S. cerevisiae*, the recognition component of the N-end rule pathway is encoded by the *UBR1* gene (10). A *ubr1* Δ mutant is viable, grows at nearly wild-type rates, but is unable to degrade N-end rule substrates, which are short-lived in wild-type (*UBR1*) cells (8, 10).

In a search for the functions of the N-end rule, we carried out a "synthetic lethal" screen to identify mutants whose viability requires the presence of the *UBR1* gene (11). To isolate such mutants, termed *sln* (synthetic lethal of N-end rule), we used a screen based on 5-fluoroorotic acid (FOA) (12). In this method, yeast cells lacking chromosomal copies of both *URA3* and a (nonessential) gene of interest are transformed with a plasmid that expresses both of these genes. The cells are mutagenized and examined for growth on plates containing FOA and uracil. Because FOA selects against *URA3*-expressing cells (12), mutants that grow in the absence but not in the presence of FOA should include those whose viability requires the plasmid carrying the gene of interest linked to *URA3*.

A synthetic lethal screen with *UBR1* yielded a recessive mutant, *sln1-1*, which was viable in the *UBR1* but not in the *ubr1* Δ background (11). Our earlier attempts to clone *SLN1* yielded *PTP2*, which encodes a putative phosphotyrosine phosphatase, and is an extragenic multicopy suppressor of *sln1-1* (11). The *SLN1* gene was isolated as described (13). That the subcloned DNA fragment containing a single open reading frame (ORF) was indeed *SLN1* (rather than an extragenic suppressor of *sln1-1*) was confirmed by linkage analysis (13). The 3.66-kb ORF of *SLN1* encodes a

Division of Biology, California Institute of Technology, Pasadena, CA 91125.

*To whom correspondence should be addressed.